International Journal of GEOMATE, July, 2020, Vol.19, Issue 71, pp. 77 - 83
ISSN: 2186-2982 (P), 2186-2990 (O), Japan, DOI: https://doi.org/10.21660/2020.71.39213
Geotechnique, Construction Materials and Environment

A MODEL FOR ASSESSMENT OF TREE STABILITY AND ENTRAINMENT OF WOODY DEBRIS BY FLOW SLIDES AND SHALLOW SLOPE FAILURE

*Thapthai Chaithong[1]

[1]Department of Geography, Faculty of Social Sciences, Kasetsart University, Thailand

*Corresponding Author, Received: 17 Aug. 2019, Revised: 21 Feb. 2020, Accepted: 29 Feb. 2020

ABSTRACT: The effect of trees on the stability of soil slopes is widely studied. Tree roots can reinforce the soil slope by increasing its shear strength; moreover, trees may reduce soil moisture content through the transpiration process, which may reduce the pore-water pressure, improving the shear strength of the soil slope. Nevertheless, trees can also be felled by landslides and flow slides. Fallen trees create woody debris, which is a serious hazard precipitated by landslides, slope failures, and flow slides that increases the magnitude of the destruction caused to infrastructure and housing. The processes of tree instability and the entrainment of woody debris are important mechanisms in the study of the behaviour of woody debris in the ecosystem. Therefore, the purpose of this study is to propose a model to describe the mechanism of tree instability caused by shallow slope failures and flow slides, including the entrainment of woody debris by flow slides or debris flows. The proposed model combines a rainfall-induced shallow slope failure model, a sliding block model for flow slides runout analysis, and a tree stability model.

Keywords: Slope failure, Tree, Root strength, Debris flow, Woody debris, Tree stability, Landslide

1. INTRODUCTION

Generally, slope mass movement can be divided into three main parts: landslide initiation, flow slide, and deposition of slope mass. The mechanism by which shallow slope failure is triggered by rainfall is the build-up of positive pore-water pressure or groundwater along the bedrock under undrained conditions. The increase in positive pore-water pressure reduces the effective stress and the shear strength. Ultimately, this can trigger initial movements in the slope mass and also lead to flow slides or rapid debris flow. Runout analysis of flow slides involves the determination of the flow velocity, flow path, the impact force of debris flows, and other factors. Shallow slope failures and flow slides can destroy large areas of mountain forest. Numerous studies have examined landslide scars and woody debris [1-3]. In addition, woody debris is frequently entrained by flow slides or debris flows, potentially threatening further trees in the path of the slide flow, before being deposited in downstream villages.

Rainfall-induced shallow slope failure and debris flow models have been proposed by numerous studies. For instance, TRIGRS for landslide analysis was proposed by the United States Geological Survey, SINMAP for slope stability index analysis was proposed by Utah State University, and DAN or RAMMS has been proposed for the runout analysis of debris flow. Moreover, numerous researchers have studied tree stability models. However, few studies have combined rainfall-induced shallow slope failure analysis, runout analysis of slide flow, and tree stability models to analyse tree stability and the entrainment of woody debris by slope mass movement. Therefore, this study proposes a model for assessing the stability of trees and the entrainment of woody debris by shallow slope failures and flow slides.

2. THEORETICAL DESCRIPTION OF RAINFALL-INDUCED SHALLOW SLOPE FAILURE MODEL, SLIDING BLOCK MODEL AND TREE STABILITY MODEL

2.1 Rainfall-induced shallow slope failure model

To model shallow slope failure induced by rainfall, the model is divided into three main parts that are used to describe the relationship among rainwater infiltration, subsurface discharge, and slope stability.

2.1.1 Rainwater infiltration model

This study uses the Green-Ampt (GA) model to calculate the amount of rainwater that infiltrates the hillslope. The GA model is a simplified infiltration model that assumes a homogeneous soil profile and a uniform initial distribution of water content. Moreover, the suction head at the wetting front and the coefficient of hydraulic conductivity are constant [4]. Mountainous areas are characterised by sloping terrain. Hence, this study uses the GA model for a sloping surface as proposed by

reference 5. Equation (1) shows the infiltration rate equation of the GA model for a sloping surface. Equation (2) shows the cumulative infiltration equation of the GA model for a sloping surface.

$$i(t) = k\left[\cos\beta + \frac{\psi_f \Delta\theta}{I(t)}\right] \quad (1)$$

$$I(t) - \frac{(\psi_f \Delta\theta)}{\cos\beta}\ln\left[1 + \frac{I(t)\cos\beta}{(\psi_f \cdot \Delta\theta)}\right] = k\cos\beta \cdot t \quad (2)$$

where $i(t)$ is the infiltration rate at time t, $I(t)$ is the cumulative infiltration at time t, ψ_f is the suction head at the wetting front, $\Delta\theta$ is the volumetric water content deficit, k is the coefficient of hydraulic conductivity and β is the slope angle.

2.1.2 Subsurface hydrological model

Groundwater recharge is based on hydrological and meteorological factors such as precipitation and temperature, as shown in Eq. (3) [6,7]:

$$R = P - Q_R - E \pm S_t \pm S_y \quad (3)$$

where R is the recharge, P is the precipitation, Q_R is the runoff, E is evapotranspiration, S_t is storage, and S_y is the synthetic elements. In this study, the mechanism of rainfall-induced shallow slope failure is based on a groundwater increase due to rainfall that reduces the shear strength of the soil slope. In the monsoon season, E and S_y will be omitted due to the continuity of precipitation; moreover, S_t is neglected for simplified calculation [7]. The runoff and infiltration are components of rainfall activity with the ground.

$$Q_R = P - I \quad (4)$$

Therefore

$$R = I \quad (5)$$

where I is the rainwater infiltration.

The groundwater discharge is based on Darcy's law, as shown in Eq. (6). The subsurface flow in the groundwater zone or saturated zone is based on the steady-state condition, and the groundwater table is parallel to the topography. In addition, the groundwater flows through a porous medium.

$$q = b \cdot m \cdot k \cdot \eta \cdot \sin\beta \quad (6)$$

where q is the subsurface discharges, b is the width, m is the water table height, and η is the porosity.

The steady-state subsurface flow to balance the groundwater recharge per contributing area is shown in Eq. 7:

$$q = I \cdot a \quad (7)$$

where a is the contributing area.

By combining Eq. (6) and Eq. (7), the water table height can be predicted using Eq. (8):

$$m = [I \cdot a] / [b \cdot m \cdot k \cdot \eta \cdot \sin\beta] \quad (8)$$

2.1.3 Infinite slope stability model

The infinite slope stability model is a traditional slope stability model utilised to analyse shallow slope failures or shallow landslides. Shallow slope failures are characterised by a shallow depth and form failure planes parallel to the hillslope surface. These factors are similar to the assumptions of the infinite slope stability model. The stability of the hillslope is presented in the form of a safety factor, as shown in Eq. (9). The safety factor is the ratio of driving stress to resisting stress. Resisting stress is developed based on the Mohr–Coulomb failure criteria.

$$Fs = \frac{(c' + c_r) + \cos\beta^2\left[m * \gamma' + (H - m)\gamma_t\right]\tan\phi'}{\cos\beta\sin\beta\left[m * \gamma_{sat} + (H - m)\gamma_t\right]} \quad (9)$$

where c' is the effective soil cohesion, c_r is the root cohesion, H is soil depth, γ_{sat} is the saturated soil unit weight, γ_t is the total soil unit weight, γ_w is the water unit weight and ϕ' is the soil friction angle.

2.2 Sliding block model

The sliding block model is a lumped mass model utilised to describe the movement of the centroid of a debris flow. To analyse sliding block motion, the acting force is a significant result of the driving force and movement resistance. In this analysis, gravity imposes a driving force and the movement resistance is developed based on a combination of Coulomb's friction law and Terzaghi's effective stress principle. The sum of the driving force and movement resistance is the net force, as shown in Eq. (10):

$$F_n = M_d \cdot g \cdot (\sin\beta) - M_d \cdot g \cdot (1 - r_u)\tan\phi\cos\beta \quad (10)$$

where F_n is the net force, M_d is the mass of debris flow, g is the gravitational acceleration, r_u is the pore pressure ratio.

In terms of the mass of debris flows, there are two main phases: solid and liquid. Generally, soil and rock are the main components of the solid phase.

The mass of the debris flow (M_d) can be calculated using Eq. (11):

$$M_d = \gamma_d V_d \tag{11}$$

where γ_d is the unit weight of debris flow, V_d is the volume of debris flow.

However, the debris flow can entrain woody material during its flow downstream. Thus, woody material also factors into the debris flow using the momentum of entrainment. Eq. (12) represents the change in flow momentum resulting from the entrainment of woody material, whereas Eq. (13) presents the momentum of the sliding block.

$$\frac{d\left(m_d v\right)}{dt} = F_n \tag{12}$$

Therefore

$$m_d \frac{dv}{dt} = F_n - v\frac{dm}{dt} \tag{13}$$

The term $-v(dm/dt)$ in Eq. (13) is the consequence of momentum conservation; dm/dt, in the case of woody material entrainment by debris flow, refers to the mass of woody debris or fallen trees entrained by the debris flow. From Eq. (13), we can write this in a dimensionless form. The momentum change is $\left(m_d + \Delta m\right)\left(v + \Delta v\right) - m_d v$. Since we neglect a second order term, we have:

$$\Delta v = \frac{F_n \Delta t - \Delta m v}{m_d} \tag{14}$$

where Δm the increment of mass during the time step that refers to woody debris entrainment by debris flow during the time step in this study. Figure 1 shows the motion of the debris flow during the time step and woody material entrainment.

Thus, the mass of the debris flow after the entrainment process can be calculated using Eq. (15):

$$M_d = \gamma_d V_d + \gamma_{wm} V_{wm} \tag{15}$$

where γ_{wm} is the unit weight of woody material, V_{wm} is the volume of woody material that is entrained by the debris flow.

The velocity in each time step can be calculated using:

$$v_{i+1} = v_i + \frac{F_n \Delta t - \Delta m v_i}{m_d} \tag{16}$$

where v_{i+1} is the velocity at time $i+1$ and v_i is the velocity at time i.

The displacement of the slide block can be calculated by Eq. (17):

$$s_{i+1} = s_i + 0.5\Delta t\left(v_i + v_{i+1}\right) \tag{17}$$

where s_{i+1} is the displacement at time $i+1$, and s_i is the displacement at time i.

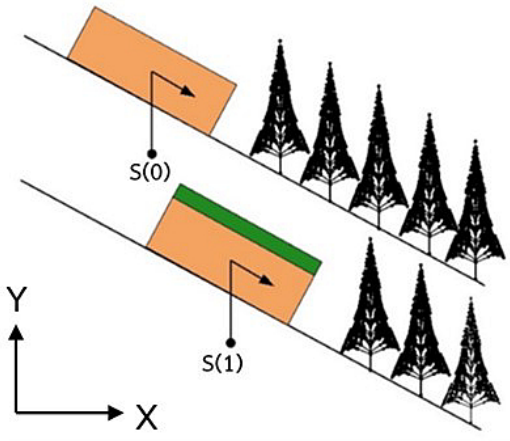

Fig.1 Motion of debris flow in time step and woody material entrainment

Three main types of force—namely hydrostatic, impact, and drag forces—assail trees as a consequence of debris flow. These are considered as shown below. [8,9]

$$F_{hs} = 0.5\gamma_d H_d{}^2 D_{tree} \tag{18}$$

$$F_{im} = k\gamma_d H_d D_{tree} v^2 \tag{19}$$

$$F_{dr} = 0.5\gamma_d v^2 H_d D_{tree} C_D \tag{20}$$

where F_{hs} is the hydrostatic force. H_d is the height of debris flow. D is the diameter of tree at breast height (DBH). k is the impact force coefficient. C_D is the drag coefficient.

2.3 Tree stability model

Based on the observations, the model of tree failure is assumed to be a soil–root failure mode. The ordinary method of slices was found to be suitable a stability model for a soil–root failure mode [10,11]. The soil–root failure mode is characterised by the failure plane passing through both the soil and the root of the tree in a semicircle or part-circle in two dimensions, moreover, in the shape of a half-cylinder and a hemisphere [12]. This study considers the case of the hemisphere shape. Moreover, the concept of shear strength is based on the Mohr–Coulomb failure criteria. Figure 2 shows the schematic of the tree stability analysis. The stability of the tree is the ratio of the resisting shear force to the driving shear force, as shown in Eq. (21).

$$Ts = \frac{R_m \tau_{s-r}}{R_m W_t + F_{hs} R_{hs} + F_{im} R_{im} + F_{dr} R_{dr}} \quad (21)$$

where *Ts* is the tree stability index. τ_{s-r} is the total shear strength of tree. R_m is the moment arm of total shear strength of tree. W_t is total weight that is the summing weight of tree and weight of soil. R_{hs} is the moment arm of hydrostatic force. R_{im} is the moment arm of impact force. R_{dr} is the moment arm of drag force.

The shear strength on the slip surface is represented by Eq. (22).

$$\tau_{s-r} = \left[C \cdot \left(2\pi r^2\right)\right] + \left[\left(\gamma_t \left(\frac{2\pi r^3}{3}\right)\cos\beta\right) - \left(\gamma_w \left(\pi H_w^2 \left(r - \frac{H_w}{3}\right)\right)\right)\right]\tan\phi' \quad (22)$$

where τ_{s-r} is the total shear strength of tree. *C* is the total cohesion (c' + c_r). *r* is the radian of hemisphere. H_w is the height of water table.

Considering to the driving force, the total weight can be calculated using Eq. (23).

$$W_t = \left[\gamma_t \sin\beta \left(\frac{2\pi r^3}{3}\right)\right] + \left[\left(V_t \gamma_{wm}\right)\sin\beta\right] \quad (23)$$

For simplified calculation, we assume that the centre of overturning is the centroid of the hemisphere in the initial moment of tree failure. Therefore, the moment arm of the total shear strength of the tree can be calculated as follows:

$$R_m = r - \left(\frac{3r}{8}\right) \quad (24)$$

where *r* is the radian of hemisphere.

The moment arm of hydrostatic force can be calculated as a following:

$$R_{hs} = \frac{1}{3}H_d + \frac{3}{8}r \quad (25)$$

The moment arm of hydrostatic force can be calculated as follows:

$$R_{im}, R_{dr} = 0.5H_d + \frac{3}{8}r \quad (26)$$

Figure 2 shows Schematic of tree stability analysis and distribution of flow slide forces which "x" in the Figure 2 is the $(3/8)r$

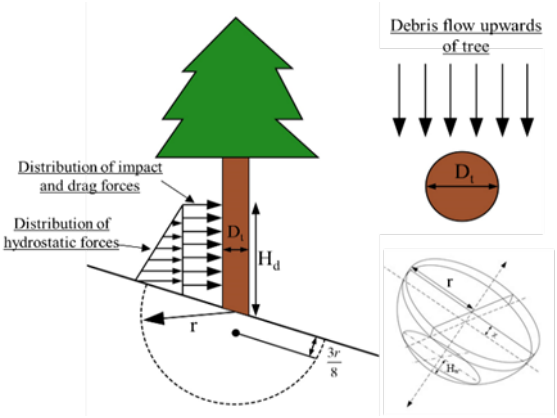

Fig.2 Schematic of tree stability analysis and distribution of flow slide forces

3. CALCULATION FRAMEWORK

There are three main parts to the calculation. First, the initial landslide is calculated using the rainfall-induced shallow slope failure model. The result of the first step is the landslide occurrence time and safety factor. The second step is to calculate the slide flow runout and velocity. Finally, the forces and tree stability are calculated using Eqs. (18-20) and the tree stability model. Table 1 summarises the parameters used in the rainfall-induced shallow slope failure, the sliding block model and the tree stability model. The parameters was collected and found by the field survey and laboratory tests. The density of woody material was approximately 3.4 kN/m^3 for Cryptomeria japonica [13].

This study examined the historical landslide and flow slide that occurred on the local slope of the town of Iwaizumi, in Japan's Iwate Prefecture, on 30 August 2016. Figure 3 shows the topography of the case study. The study analysed three locations to calculate the stability of the trees during the debris flow and deposition.

Table 1 Infiltration parameters, soil and wood properties used in this study

Parameters	Unit	Values
Hydraulic conductivity	m/hr	0.03
Volumetric water content deficit	-	0.16
Suction head at wetting front	m	0.022
Total unit weight of soil	kN/m^3	14.40
Soil cohesion	kN/m^2	5.6
Root cohesion	kN/m^2	3.2
Unit weight of water	kN/m^3	9.81
Soil friction angle	degrees	24.7
Diameter of tree	m	0.24
Unit weight of debris flow	kN/m^3	24.06
Slope angle 1, β_1	degrees	22.38
Slope angle 2, β_2	degrees	14.04
Slope angle 3, β_3	degrees	5.43

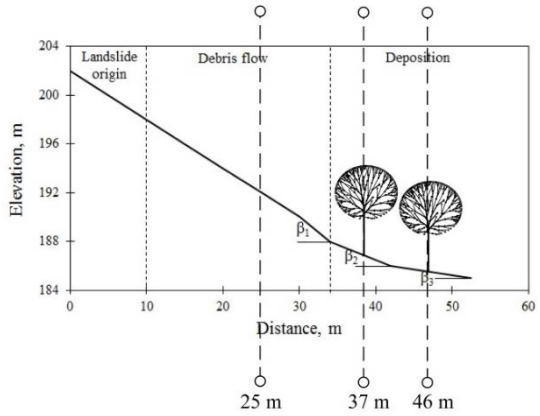

Fig. 3 Topography and elevation of case study.

4. RESULTS AND DISCUSSION

Considering the initiation location of landslide, shallow slope failure located at the top of the hillslope (slope angle 1). Figure 4 plots the safety factor and hourly rainfall on 30 August 2016. In this study, we used the rainfall data measured and collected at the Iwaizumi rain gauge operated and provided by Japan Meteorological agency and Iwate prefecture, Japan because the Iwaizumi rain gauge was installed in closest proximity to our study area. The peak hourly rainfall of 63 mm was collected and recorded at 18:00 on 30 August 2016. Total 24 hour rainfall at Iwaizumi rain gauge was approximately 200 mm. According to our computations, we found that the safety factor of the hillslope was less than 1 between 17:00 and 18:00 on 30 August 2016. The cumulative rainfall during the period when the safety factor was less than 1 was approximately 160 mm. The safety factor slightly declined at the beginning of rainfall because the amount of rainfall was low intensity. The high intensity rainfall started at 16:00 on 30 August 2016, hence, the factor of safety rapidly decreased at this time (Figure 4).

Figure 5 shows the plot of the relation between the velocity of the flow slide and time. Figure 6 shows the plots of the relation between the velocity of the flow slide and horizontal displacement. The plots show that the velocity of the flow slide increased at slope angle 1 and almost constant at slope angle 2. The velocity of the flow slide decreased at slope angle 3. The flow slide stopped and deposited its debris at a horizontal distance of 47 m. The location of the deposition based on the calculation accords well with our field observations at the site. According to the calculation, the total duration of the flow slide from the origin of the landslide to deposition was approximately 28 seconds.

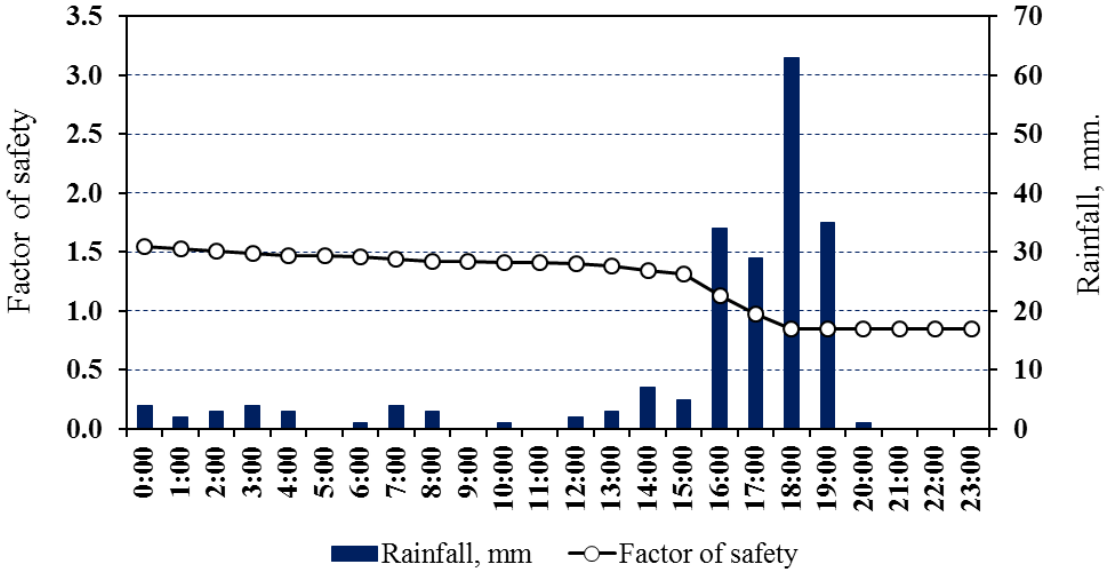

Fig.4 Safety factor of case study and hourly rainfall at Iwaizumi rain gauge.

Figure 5 shows the plot of the relation between the velocity of the flow slide and time. Figure 6 shows the plots of the relation between the velocity of the flow slide and horizontal displacement. The plots show that the velocity of the flow slide increased at slope angle 1 and decreased slightly at slope angle 2. The velocity of the flow slide sharply decreased at slope angle 3. The flow slide stopped and deposited its debris at a horizontal distance of 51 m. The location of the deposition based on the calculation accords well with our field observations at the site. According to the calculation, the total duration of the flow slide from the origin of the landslide to deposition was approximately 8 seconds. Figure 7 shows a photograph of the site studied in this research.

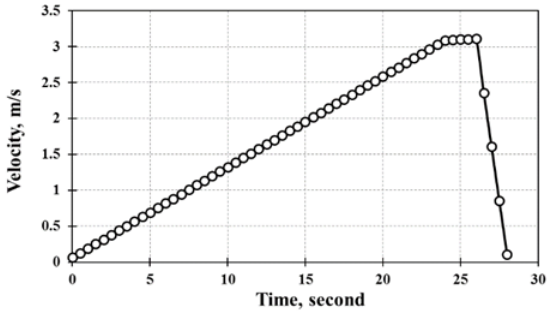

Fig. 5 Velocity of flow slide versus time.

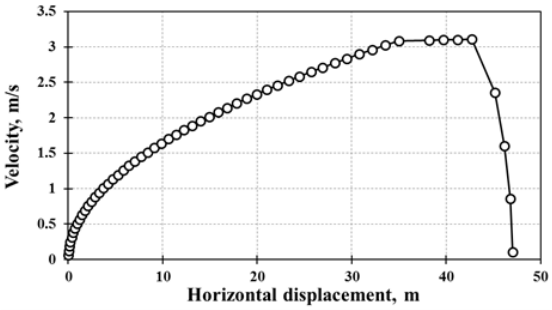

Fig. 6 Velocity of flow slide versus horizontal displacement.

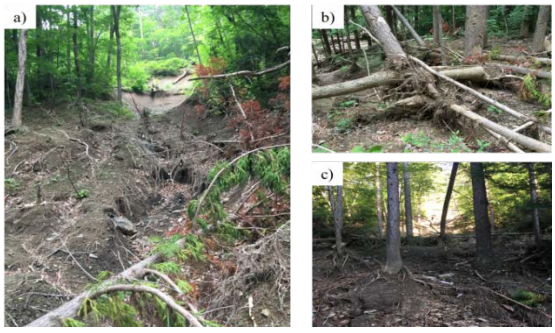

Fig. 7 a) Origin of landslide; b) the condition of trees at 37 m; and c) the condition of trees at 46 m.

Tree stability was calculated at three slope locations at the horizontal distances of 25 m, 37 m, and 46 m. The calculation showed a tree stability index of less than 1 at a horizontal distance of 25 m, which agrees well with our field observations. At a horizontal distance of 37 m, the results of the calculation showed a tree stability index of approximately 1. In addition, the tree stability index at 46 m was approximately 1.7. Field observations revealed that the trees at a horizontal distance of 25 m had been felled. Trees at a horizontal distance of 37 m were nearly toppled, and trees at 46 m remained standing.

5. CONCLUSION

An integrated model was designed that could analyse tree stability on the hillslope. The results of the model are a good fit for the data obtained from the field observation. The unknown factors of tree and soil parameters are critical variables in the calculation. The diameter of tree is the critical parameter because the diameter of tree is high uncertainty. The soil parameters are also the critical variable because they need to obtain from the testing. Moreover, in developing a two-dimensional model, a significant challenge is posed by simulating the woody debris recruitment caused by shallow slope failures or landslides.

REFERENCES

[1] Chaithong T., Komori D., Sukegawa Y., Touge Y., Mitobe Y., Anzai S., Landslides and Precipitation characteristics during the Typhoon Lionrock in Iwate Prefecture, Japan. International Journal of GEOMATE, Vol. 14, Issue 44, 2018, pp.109-114.

[2] Soralump S., Disastrous Landslides at Khao Panom, Krabi, Thailand. Conference proceedings, in Proc. EIT-JAPAN Symposium 2011 on Human Security Engineering. 2011.

[3] Ruiz-villanueva V., Diez-herrero A., Ballesteros J. A., Bodoque J. M., Potential Large Woody Debris Recruitment due to Landslides, Bank Erosion, and Floods in Mountain Basins: A Quantitative Estimation Approach. RIVER RESEARCH AND APPLICATIONS, Vol. 30, 2014, pp.81-97.

[4] Muntohar A. S. and Liao H. J., Analysis of Rainfall-induced Infinite Slope Failure during Typhoon using a Hydrological-geotechnical Model. Environ Geol, Vol 56, Issue 1161, 2009.

[5] Chen L. and Young M. H., Green-Ampt Infiltration Model for Sloping Surfaces. WATER RESOURCES RESEARCH, Vol. 42, 2006, pp.1-9.

[6] Sengrey D., Harrop-Williams K. O. and Klaiber J. A., Predicting Ground-water Response to Precipitation. Journal of Geotechnical Engineering, Vol. 110, 1984, pp.957-975.

[7] Kim J., Lee K., Jeong S. and Kim G., GIS-based Prediction Method of Landslide Susceptibility using a Rainfall Infiltration-groundwater flow Model. Engineering Geology, Vol. 182, 2014, pp.63-78.

[8] Gao L., Zhang L. M. and Chen H. X., Two-dimensional Simulation of Debris Flow Impact Pressures on Building. Engineering Geology, Vol. 226, 2017, pp.236-244.

[9] He S., Liu W. and Li X., Prediction of Impact Force of Debris Flows Based on Distribution and Size of Particles. Environ Earth Sci, Vol. 75, Issue 298, 2016.

[10] Rahardjo H., Amalia N., Leong E. C., Harnas F. R., Tieng L. T. and Fong Y. K., Flux Boundary Measurements for the Study of Tree

Stability. Landscape Ecol Eng, Vol 13, 2017, pp.81-92.

[11] Rahardjo H., Harnas F. R., Leong E. C., Tan P. Y., Fong Y. K. and Sim E. K., Tree Stability in an Improved Soil to Withstand Wind Loading. Urban Forestry & Urban Greening, Vol 8, 2009, pp.237-247.

[12] Bartelt P. and Stockli V., The Influence of Tree and Branch Fracture, Overturning and Debris Entrainment on Snow Avalanche Flow.

[13] Annals of Glacilogy, Vol. 32, 2001, pp.209-216. Takeshi F., Kana Y. and Katsushi K., Basic densities as a parameter for estimating the amount of carbon removal by forests and their variation. Bulletin of FFPRI, Vol.6, No.4, 2007, pp.215-226.